Article

Not peer-reviewed version

Selective Capture and Continuous Recovery of Sulfur-Containing Molecules from Flowing Wastewater Using a Capillary $Ag_2Mo_3O_{10}·1.8H_2O$/Carbon Fiber Membrane System

Leiyang Xue , Chuya Luo , Hanmei Xu , Jiaxin Hua , Xue Zhang , Lianwen Zhu * , Jun Wu *

Posted Date: 30 December 2025

doi: 10.20944/preprints202512.2569.v1

Keywords: $Ag_2Mo_3O_{10}·1.8H_2O$/carbon hybrid framework; capillary-driven separation; selective adsorption; continuous resource recovery

 doi:10.20944/preprints202512.2569.v1

Article

Selective Capture and Continuous Recovery of Sulfur-Containing Molecules from Flowing Wastewater Using a Capillary $Ag_2Mo_3O_{10}·1.8H_2O$/Carbon Fiber Membrane System

Leiyang Xue [1], Chuya Luo [1], Hanmei Xu [1], Jiaxin Hua [1], Xue Zhang [1], Lianwen Zhu [1,*] and Jun Wu [2,*]

[1] School of Biology and Chemical Engineering, Jiaxing University, Jiaxing 314001, China; College of Engineering of Biology and Chemistry, Jiaxing University, Jiaxing 314000, China

[2] College of Advanced Materials Engineering, Jiaxing Nanhu University, Jiaxing 314001, China

* Correspondence: lwzhu@zjxu.edu.cn (L.Z.); wujun@jxnhu.edu.cn (J.W.)

Abstract

This study presents a novel membrane-inspired $Ag_2Mo_3O_{10}·1.8H_2O$/carbon fiber cloth (CFC) hybrid framework designed for the continuous and selective recovery of high-value sulfur-containing molecules from organic wastewater. The framework was fabricated by uniformly growing $Ag_2Mo_3O_{10}·1.8H_2O$ nanowires on CFC membrane, forming a hierarchical porous network with abundant micro-nano channels that facilitate efficient, capillary-driven water transport. Owing to its mesoporous structure and specific Ag-S coordination affinity, the material exhibits excellent selectivity for sulfur-containing dyes, achieving rapid adsorption (>94% removal of methylene blue within 10 minutes) and high specificity in mixed solutions. Moreover, the hybrid framework demonstrates outstanding reusability, retaining high recovery efficiency over multiple cycles. A continuous-flow system based on this framework operates without external pressure and achieves a water transport rate of 1875 $mL·h^{-1}·m^{-2}$. These results underscore the potential of the $Ag_2Mo_3O_{10}·1.8H_2O$/CFC system as an efficient, scalable, and sustainable platform for industrial wastewater resource recovery.

Keywords: $Ag_2Mo_3O_{10}·1.8H_2O$/carbon hybrid framework; capillary-driven separation; selective adsorption; continuous resource recovery

1. Introduction

Water resources are vital for sustaining human life and societal development. However, significant pressures on aquatic ecosystems—including structural challenges, root causes, and persistent trends—continue to intensify, with nutrient pollution (e.g., from nitrogen and phosphorus) becoming increasingly prominent [1,2]. Beyond mere purification, resource-oriented treatment of organic wastewater holds greater long-term significance, transforming pollutants into recoverable materials. This approach, often termed wastewater resource recovery, involves directing industrial, agricultural, and domestic effluents through tailored purification systems that employ physical, chemical, or biological methods to meet reuse standards [2]. For example, integrated treatment strategies combining membrane separation, adsorption, and Fenton oxidation have been developed for the remediation of printing and dyeing wastewater [3].

Adsorption is a simple, flexible, and economical approach for treating dye wastewater, making it one of the most effective and practical methods for removing toxic substances [4]. Physical adsorption works well for low-concentration soluble dyes, but conventional adsorbents often suffer from limited capacity, poor selectivity, lack of resource recovery, regeneration challenges, and low

 doi:10.20944/preprints202512.2569.v1

reuse rates. Membrane technology has advanced significantly due to its high efficiency, cost-effectiveness, eco-friendliness, and potential for achieve "Zero Liquid Discharge"[5,6]. However, membrane processes are often hampered by high operation and maintenance costs, energy consumption, and fouling. Other chemical processes such as photocatalytic oxidation, are limited by insufficient purification capacity and complex operational requirements [7,8]. From a practical standpoint, an ideal organic wastewater resource recovery system should be simple, efficient, economical, durable, and environmentally friendly, while also enabling (1) resource utilization; (2) continuous operation; and (3) selective separation capability. Therefore, developing new materials and technologies for water purification and resource recovery remains a critical research focus [9].

In recent years, micro/nano-structured layered oxide composites have garnered significant attention in the fields of adsorption and membrane separation owing to their hierarchical architecture [10–14], facile functionalizability, well-defined transport channels, high specific surface area, fully accessible active sites, and excellent stability. Their selective adsorption performance can be precisely tailored through various synthetic strategies-including hydrothermal/solvothermal, co-precipitation, templating, and polymerization methods-as well as via selective mechanisms such as molecular/ion imprinting, surface charge modulation, hard–soft acid–base interactions, synergistic effects, and specific surface functionalization [15]. This versatility supports the hypothesis that integrating layered oxides with complementary composite components can yield materials with enhanced and tunable selective adsorption functionality.

The crystal structure of $Ag_2Mo_3O_{10}\cdot1.8H_2O$ consists of a layered structure composed of zigzag chains of edge-sharing molybdenum-oxygen hexagonal octahedra, interconnected via interlayer silver ions. Since silver ions readily form Ag-S bonds, the interlayer silver ions in $Ag_2Mo_3O_{10}\cdot1.8H_2O$ nanowires can selectively adsorb sulfur-containing organic dyes via coordination bonds, enabling selective separation of mixed dyes without complex surface modification[16,17]. Inspired by the principles of membrane separation processes, we propose to grow $Ag_2Mo_3O_{10}\cdot1.8H_2O$ nanowires directly on a flexible and porous membrane substrate, thereby constructing a continuous, integrated separation system. This approach effectively combines the selective adsorption capability of layered oxide composites with the structural and functional advantages of membrane technology, enabling simultaneous molecular recognition and continuous fluid transport. Such a design not only enhances separation efficiency but also aligns with the scalable and modular nature of modern membrane systems, offering a promising pathway toward advanced functional membranes for targeted resource recovery.

In this work, we developed a membrane-inspired continuous-flow resource recovery system based on an $Ag_2Mo_3O_{10}\cdot1.8H_2O$/carbon fiber cloth (CFC) hybrid framework. By growing $Ag_2Mo_3O_{10}\cdot1.8H_2O$ nanowires uniformly on a large-area CFC substrate, we constructed an integrated porous network that mimics the structural and functional principles of separation membranes. This framework combines molecular-level selectivity through Ag-S coordination bonds with passive, capillary-driven transport analogous to membrane permeation, enabling energy-efficient and continuous operation. The system not only achieves rapid and specific adsorption of methylene blue from mixed dye solutions but also demonstrates excellent reusability, maintaining ~97% recovery efficiency over multiple cycles. Thus, this work presents a membrane-inspired platform for selective, continuous, and sustainable recovery of high-value molecules from wastewater streams.

2. Materials and Methods

2.1. Experimental Details Materials

Carbon fiber cloth (CFC) was commercially available (purchased from Yixing Xingtan Composite Material Co., Ltd.). $AgNO_3$(Sinopharm Chemical Reagent Co., Ltd., AR, ≥99.8%), $(NH_4)_6Mo_7O_{24}\cdot4H_2O$, (Shandong Keyuan Biochemical Co., Ltd., AR, ≥99%), HNO_3(Shanghai Lingfeng Chemical Reagent Co., Ltd., 65%), Methylene Blue (MB, Sinopharm Chemical Reagent Co., Ltd., 98%), Rhodamine B (RhB, Sinopharm Chemical Reagent Co., Ltd., 98%), Ethanol (Sinopharm Chemical

 doi:10.20944/preprints202512.2569.v1

Reagent Co., Ltd., AR, ≥99.7%), n-Propanol (Shanghai Macklin Biochemical Technology Co., Ltd., AR, ≥99%). The water used was deionized water.

2.2. Preparation of a $Ag_2Mo_3O_{10}·1.8H_2O$ /Carbon Framework

0.24 g of $AgNO_3$ was added to 12 mL of water to prepare a $AgNO_3$ solution; 0.465 g of $(NH_4)_6Mo_7O_{24}·4H_2O$ was dissolved in 18 mL of water to prepare an $(NH_4)_6Mo_7O_{24}·4H_2O$ solution. The $AgNO_3$ solution was poured into the $(NH_4)_6Mo_7O_{24}·4H_2O$ solution, and the mixture was stirred uniformly under ultrasonic conditions. Then, the pH of the resulting precursor solution was adjusted to 2 using 1 mol•L^{-1} HNO_3. A piece of CFC (4 cm × 20 cm) was curled and placed in a Teflon-lined autoclave, into which the precursor solution was poured. The hydrothermal reaction was conducted at 110 °C for 1 hour. To increase the loading amount of $Ag_2Mo_3O_{10}·1.8H_2O$, the hydrothermal growth process was repeated twice. After cooling to room temperature, the modified CFC was rinsed with deionized water until neutral and dried under vacuum at 80 °C.

2.3. Characterization

The morphology and structure of the samples were examined using a Hitachi S-4800 field emission scanning electron microscope (SEM). Transmission electron microscopy (TEM) and high-angle annular dark-field scanning transmission electron microscopy (HAADF-STEM) tests were performed using an FEI Tecnai G20 electron microscope. For TEM samples, $Ag_2Mo_3O_{10}·1.8H_2O$ was dispersed in ethanol via ultrasonic treatment, and the TEM samples were prepared by dropping the diluted suspension onto carbon-coated copper grids. UV-Vis-NIR reflectance spectra were recorded using an Agilent Australia Carry-5000 spectrophotometer. Raman spectra were measured using a HORIBA Scientific LabRAM Aramis Raman spectrometer (model HORIBA Scientific LabRAM HR Evolution, wavenumber range 50-4000 cm^{-1}, excitation wavelength 532 nm). UV-Vis absorption spectra were recorded using a Shimadzu UV-2550 spectrophotometer.

2.4. Water Purification and Resource Utilization Test

To demonstrate the application of the hybrid framework in water purification and resource utilization, we used Methylene Blue (MB) solution with a concentration of 10 mg•L^{-1} as model wastewater. First, we studied the adsorption performance of $Ag_2Mo_3O_{10}·1.8H_2O$. The $Ag_2Mo_3O_{10}·1.8H_2O$ obtained after the hydrothermal reaction was placed in a suction filtration device, rinsed, and then dried at low temperature in a vacuum oven. After 24 hours, it was taken out from the vacuum oven, ground into a powder form using a mortar, 0.05 g of the powder was immersed in 30 mL of MB solution and stirred. Every 5 minutes, 3 mL of the supernatant was taken, centrifuged, and the absorbance was detected at a wavelength of 664 nm using a UV-Vis spectrophotometer (Shimadzu UV-2550) to measure the concentration change of the MB solution. The specific adsorption capacity of the 0.05 g $Ag_2Mo_3O_{10}·1.8H_2O$ powder at corresponding times was calculated.

Secondly, we studied the selective adsorption performance of the hybrid framework. A piece of $Ag_2Mo_3O_{10}·1.8H_2O$/carbon hybrid framework (5 cm × 3 cm) was placed in a 200 mL glass beaker containing 50 mL of MB and Rhodamine B (RhB) mixed solution. The solution was left standing in the dark for 12 hours, and then the mixed pollutant concentration was monitored using a UV-Vis spectrophotometer.

The continuous flow water transport and resource recovery system consisted of a piece of $Ag_2Mo_3O_{10}·1.8H_2O$/carbon hybrid framework (4 cm × 12 cm) and two beakers (200 mL and 100 mL). One end of the $Ag_2Mo_3O_{10}·1.8H_2O$/carbon hybrid framework was immersed in a large beaker (200 mL) containing the MB/RhB mixed solution, and the other end was attached to the inner wall of an empty small beaker (100 mL). Driven by capillary force, the mixed solution continuously flows along the $Ag_2Mo_3O_{10}·1.8H_2O$/carbon hybrid framework. During the water transport process, Rhodamine B molecules are continuously transported, while Methylene Blue molecules are continuously captured.

 doi:10.20944/preprints202512.2569.v1

Thus, high-value molecules are continuously recovered during the water transport process. The concentration of the mixed solution was monitored using a UV-Vis spectrophotometer.

3. Results and Discussion

3.1. Formation of the $Ag_2Mo_3O_{10}·1.8H_2O$ /CFC Framework

CFC exhibits a robust skeletal framework characterized by high mechanical strength, exceptional thermal stability, and notable corrosion resistance [18,19]. The alignment of its fiber bundles creates well-defined linear nanochannels between adjacent carbon fibers, forming an ordered network of nanofluidic pathways. The pronounced capillary forces within these channels, coupled with the intrinsic hydrophobicity of the carbon fiber matrix, establish an effective platform for the generation and sustained transport of continuous water columns [20,29]. Experimental water transport measurements reveal that a CFC sample measuring 4 cm × 12 cm achieves a transport rate of up to 2188 $mL•h^{-1}•m^{-2}$, confirming its high efficiency in fluid conveyance. Based on these structural and functional advantages, CFC was selected as the scaffold material for the construction of the $Ag_2Mo_3O_{10}·1.8H_2O$/carbon hybrid system.

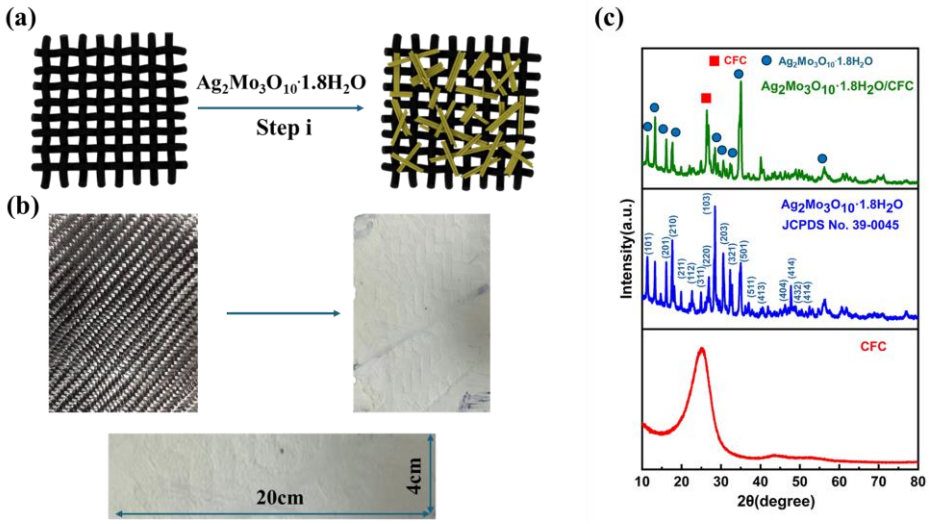

Figure 1. (a) Schematic illustration of the fabrication of $Ag_2Mo_3O_{10}·1.8H_2O$/CFC. (b) Photographs of pristine CFC and $Ag_2Mo_3O_{10}·1.8H_2O$/CFC. (c) XRD patterns of the products.

As depicted schematically in Figure 1a, the $Ag_2Mo_3O_{10}·1.8H_2O$/CFC composite was fabricated via a one-step hydrothermal process (step i, Figure 1a), in which $Ag_2Mo_3O_{10}·1.8H_2O$ nanowires were directly grown on the CFC substrate. To enhance the nanowire loading density, the hydrothermal treatment was performed twice-a critical step for achieving uniform, high-density, and large-area coverage of nanowires on the CFC support, thereby ensuring optimal functional performance of the resulting hybrid material. A representative sample of the $Ag_2Mo_3O_{10}·1.8H_2O$/carbon fiber composite, with an area of 80 cm^2, is presented in Figure 1b. The dimensions and geometry of this composite can be readily tailored to meet specific application requirements, while the $Ag_2Mo_3O_{10}·1.8H_2O$ phase demonstrates the ability to nucleate and grow uniformly over large areas of the CFC substrate with high density. After two successive hydrothermal treatments, the mass loading of $Ag_2Mo_3O_{10}·1.8H_2O$ reached 20 $mg•cm^{-2}$, suggesting its feasibility for scalable industrial implementation.

Structural analysis via XRD further confirms the successful formation of the hybrid system (Figure 1c). Prior to nanowire growth, the diffraction peak observed at 25.2° corresponds to the characteristic (002) reflection of the carbon fiber substrate, in agreement with previously reported data [19]. Following the hydrothermal synthesis, a series of distinct new diffraction peaks emerge at 11.4°, 13.3°, 16.1°, 17.7°, 28.5°, 31°, and 35°, in addition to the residual CFC signal. These additional

 doi:10.20944/preprints202512.2569.v1

peaks align well with the reference diffraction patterns of crystalline $Ag_2Mo_3O_{10}·1.8H_2O$ [21–23], confirming the successful integration of $Ag_2Mo_3O_{10}·1.8H_2O$ with the carbon fiber matrix and the establishment of a well-defined binary composite system.

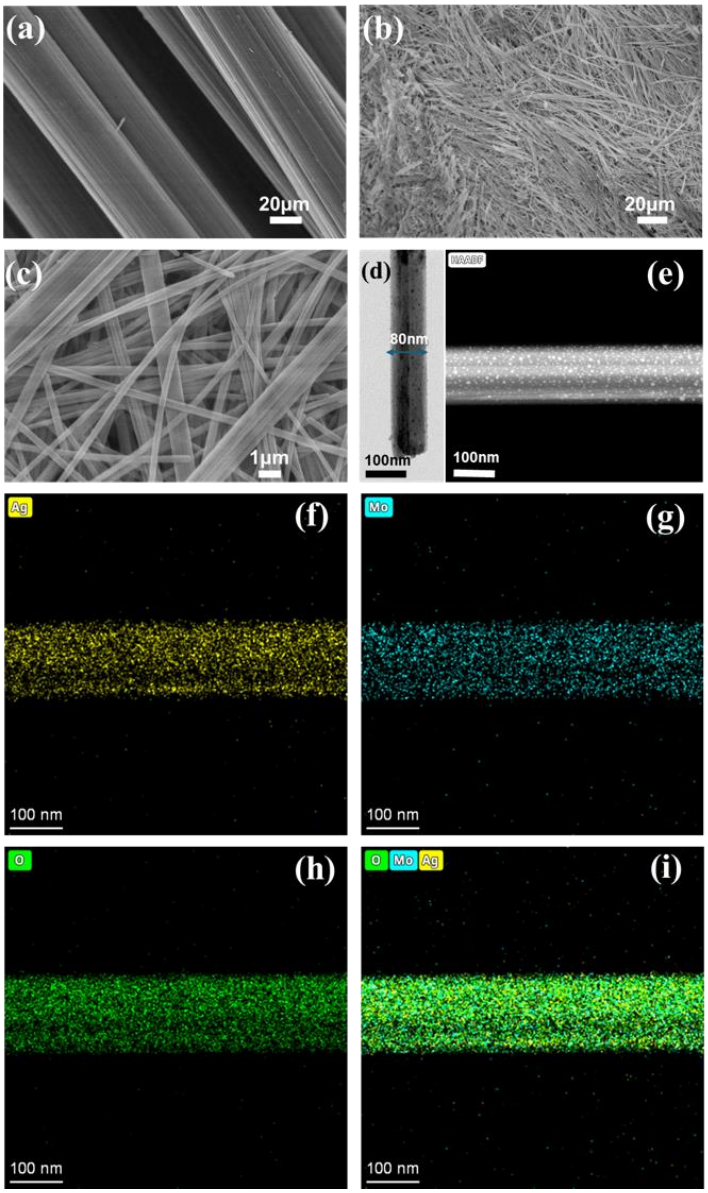

Figure 2. (a) SEM images of CFC. (b–c) SEM images of $Ag_2Mo_3O_{10}·1.8H_2O$/CFC. (d) TEM image of an individual $Ag_2Mo_3O_{10}·1.8H_2O$ nanowire. (e–i) HAADF-STEM images of the $Ag_2Mo_3O_{10}·1.8H_2O$ nanofiber (left column) and element-sensitive mapping.

The SEM image in Figure 2a illustrates the surface morphology of the CFC cloth, revealing an interwoven network of ultralong carbon fiber bundles. With an approximate thickness of 60 μm, these bundles provide a robust and scalable scaffold for the extensive deposition of $Ag_2Mo_3O_{10}·1.8H_2O$. Figures 2b-c further present the surface morphology of the $Ag_2Mo_3O_{10}·1.8H_2O$/CFC composite, demonstrating that the grown nanowires not only cover the outer surface of the CFC but also penetrate deeply into its interior, forming an interlocking network with the underlying carbon fibers [24,25]. As shown in the TEM image (Figure 2d), individual nanowires exhibit a uniform width of approximately 80 nm. These one-dimensional nanostructures interpenetrate and overlap, creating an integrated porous architecture with abundant interconnected micro- and nano-scale channels, which serve as effective pathways for capillary-driven fluid transport. Water transport measurements conducted on a 4 cm × 12 cm $Ag_2Mo_3O_{10}·1.8H_2O$/CFC sample revealed a water transport rate of 1875

 doi:10.20944/preprints202512.2569.v1

mL·h^{-1}·m^{-2}, reflecting a reduction of 313 mL·h^{-1}·m^{-2} compared to pristine CFC, likely due to the partial occupation of pores by the nanowire network.

To further confirm the composition and structure of the nanowires, HAADF-STEM and elemental mapping analyses were performed. As demonstrated in Figure 2e–i, these techniques provide atomic-scale visualization of elemental distribution, with image contrast approximately scaling with the square of the atomic number Z. Within the $Ag_2Mo_3O_{10}·1.8H_2O$ nanowires, regions corresponding to silver (Z=47) appear distinctly brighter compared to those of molybdenum (Z=42) and oxygen (Z=8), consistent with the expected compositional variation [9,26]. Combined with XRD results, these observations confirm that the nanowires consist of crystalline silver trimolybdate hydrate ($Ag_2Mo_3O_{10}·1.8H_2O$).

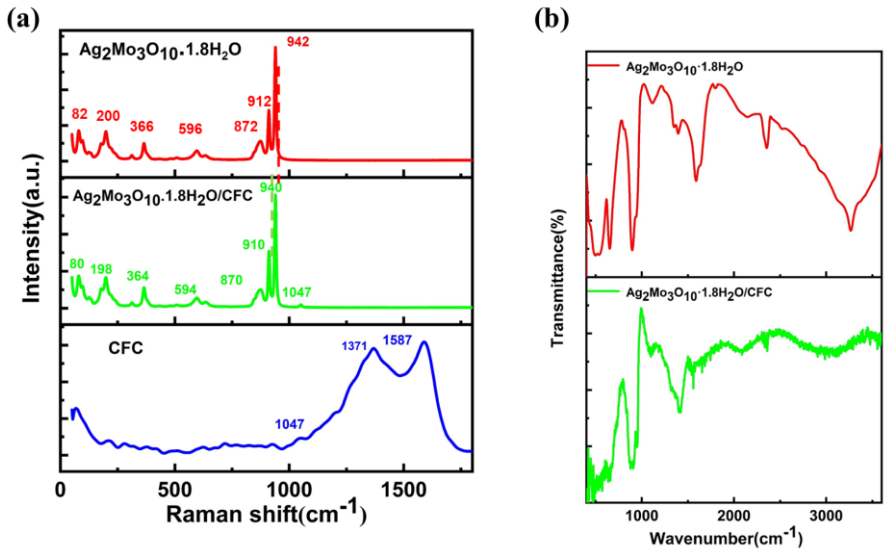

Figure 3. (a) Raman spectra of pristine carbon framework, $Ag_2Mo_3O_{10}·1.8H_2O$ and $Ag_2Mo_3O_{10}·1.8H_2O$/carbon hybrid framework. (b) Diffuse reflectance spectra for $Ag_2Mo_3O_{10}·1.8H_2O$ and $Ag_2Mo_3O_{10}·1.8H_2O$/carbon hybrid framework.

Figure 3a displays the corresponding Raman spectra. The peaks at 1371 and 1587 cm^{-1} correspond to the D and G bands of carbon fibers, respectively. Characteristic peaks of $Ag_2Mo_3O_{10}·1.8H_2O$ are observed at 940, 910, 870, 364, and 198 cm^{-1}, assigned to the stretching vibrations of MoO_4^{2-} units and bending modes of O-Mo-O bonds [30]. The high intensity of these peaks suggests a well-crystallized and densely grown nanowire phase. In the $Ag_2Mo_3O_{10}·1.8H_2O$/CFC composite, subtle but consistent shifts in the Mo-O related Raman peaks suggest interfacial interaction between the two components.Complementary IR spectra (Figure 3b) further support this interaction. The O-H stretching band shifts from around 3300 cm^{-1} in pure $Ag_2Mo_3O_{10}·1.8H_2O$ to approximately 3000 cm^{-1} in the composite. This shift, along with retained characteristic vibrational features between 500–1000 cm^{-1}, indicates structural integration likely mediated by hydrogen bonding between surface hydroxyl/carboxyl groups on the carbon fiber cloth and the crystalline water in $Ag_2Mo_3O_{10}·1.8H_2O$. Together, the Raman and IR analyses confirm a clear interfacial interaction, most probably through hydrogen bonding, facilitating structural coupling in the hybrid material.

 doi:10.20944/preprints202512.2569.v1

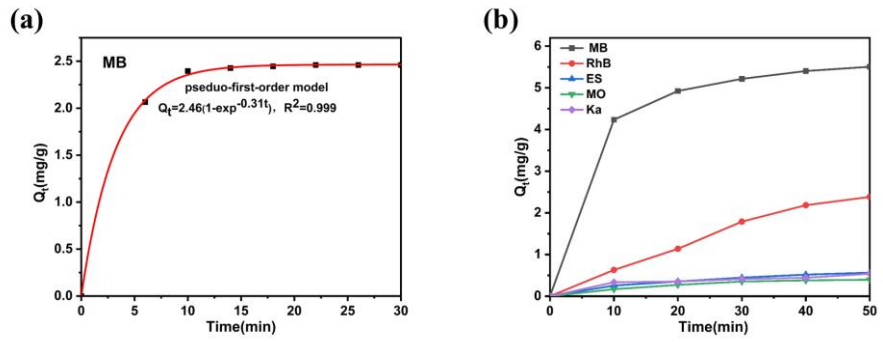

Figure 4. (a) Adsorption isotherm of pristine $Ag_2Mo_3O_{10}·1.8H_2O$ adsorption of MB. (b) The adsorption of $Ag_2Mo_3O_{10}·1.8H_2O$/carbon hybrid framework of five different organic dyes.

The adsorption performance of $Ag_2Mo_3O_{10}·1.8H_2O$ was evaluated using 10 mg/L methylene blue (MB) as a model contaminant (Figure 4a). Rapid initial uptake occurred on the external nanowire surfaces, followed by slower diffusion into the mesoporous interior. The adsorption kinetics fit pseudo-first-order model, achieving 94% MB removal within 10 minutes , indicating efficient and fast adsorption. To assess selectivity, the $Ag_2Mo_3O_{10}·1.8H_2O$/CFC composite was tested against a series of dyes including Methylene Blue (MB), Rhodamine B (RhB), Evans Blue (EB), Methyl Orange (MO), and Acidic K (Ka), each at 10 mg/L (Figure 4b). While strong and rapid adsorption was observed for MB, only minimal uptake occurred for the other dyes, including RhB, which showed only weak physical adsorption likely attributed to the carbon fiber substrate. This result clearly demonstrates the high and selective adsorption capability of $Ag_2Mo_3O_{10}·1.8H_2O$ toward methylene blue.

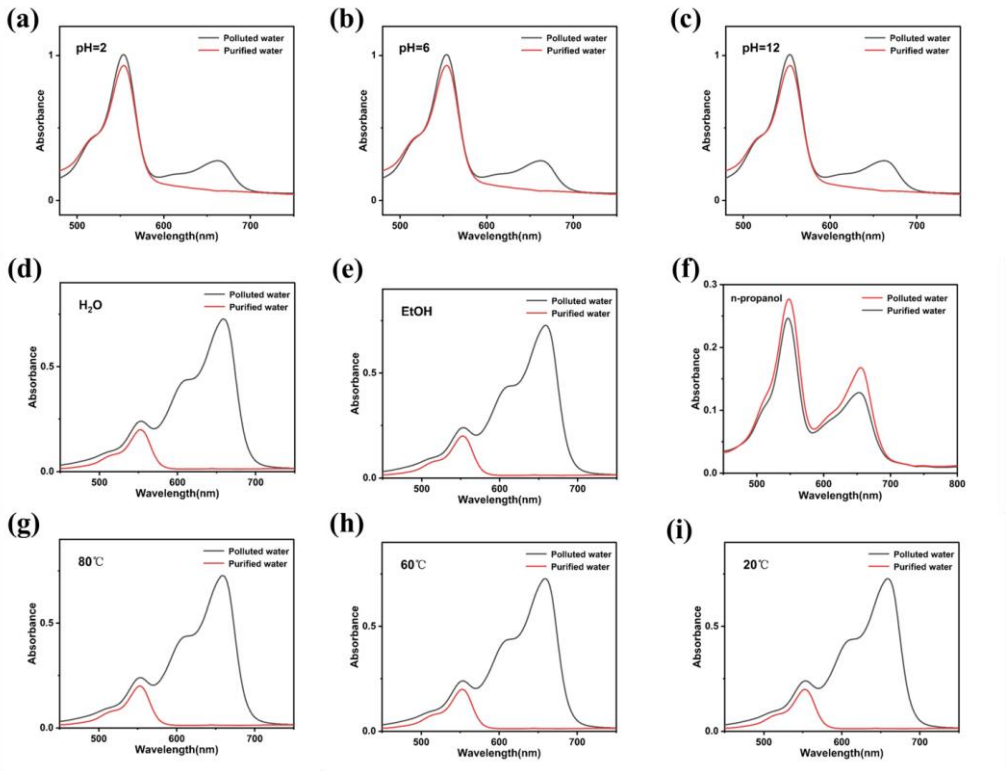

Figure 5. (a-i) UV-Vis absorption spectra of $Ag_2Mo_3O_{10}·1.8H_2O$/CFC for flow water resource recovery testing of mixed dyes (MB and RhB) in different environments (pH, solvent, and temperature). (i) Curve of the recovery ratio of MB/RhB versus reuse times of $Ag_2Mo_3O_{10}·1.8H_2O$/CFC.

 doi:10.20944/preprints202512.2569.v1

The hybrid framework was further applied in a continuous water transport configuration using mixed MB/RhB solutions. Under varying pH conditions (Figure 5a–c), the MB absorption peak at 663 nm was completely absent in the filtrate, indicating near-quantitative removal (>99%). In contrast, only about 10% of RhB was retained, consistent with weak physical adsorption within the mesoporous network. The composite also demonstrated high MB capture efficiency (>99%) in both aqueous and ethanolic MB/RhB mixtures (Figure 5d–f), whereas in n-propanol, the capture rate dropped to 32%, likely due to competitive dehydrogenation reactions catalyzed by surface Ag sites. Moreover, the material maintained stable separation performance across a range of temperatures (Figure 5g–i), confirming its thermal robustness and consistent selectivity under different environmental conditions.

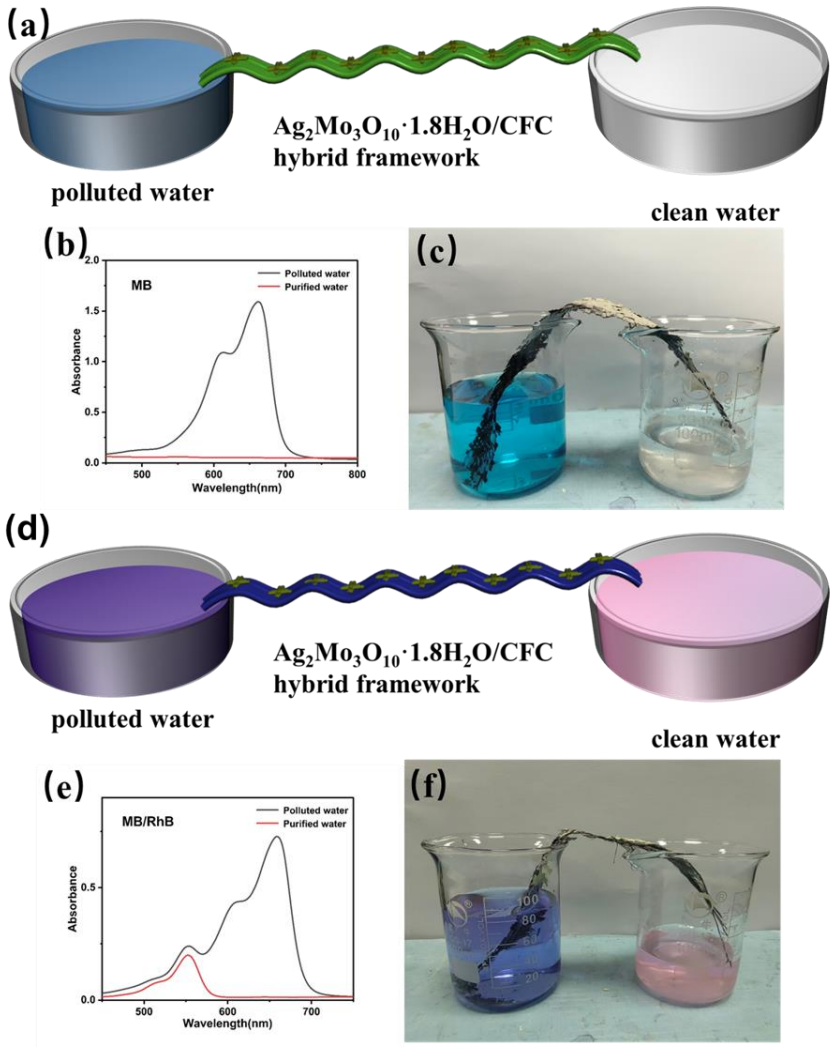

Figure 6. (a,d) Schematic diagram of the continuous flow water resource recovery system. (b, e) UV-Vis absorption spectra of polluted water and purified water. (c, f) Digital photograph of the continuous flow water resource recovery system.

The above findings demonstrate that the $Ag_2Mo_3O_{10}·1.8H_2O$/CFC hybrid framework combines rapid selective adsorption, structural stability, and scalability, underscoring its strong potential as a functional material for water resource recovery. The interconnected porous network and well-defined capillary channels inherent to the hybrid architecture provide efficient nanofluidic pathways for continuous, capillary-driven water transport. Figure 6a illustrates a continuous-flow water purification system based on the $Ag_2Mo_3O_{10}·1.8H_2O$/CFC hybrid framework. One end of the framework is immersed in a methylene blue (MB) solution, while the other end is connected to an

 doi:10.20944/preprints202512.2569.v1

empty collection vessel. Driven solely by capillary forces, the dye solution is drawn upward through the material. During transport, MB molecules are rapidly and selectively captured by the $Ag_2Mo_3O_{10}·1.8H_2O$ nanowires, resulting in only clean water reaching the collection vessel. This effective purification is confirmed by both visual observation and UV-Vis absorption spectra, which show the complete disappearance of the MB characteristic peak in the collected water (Figure 6b,c). Remarkably, when an MB/Rhodamine B (RhB) mixed solution is used as the feed, the system demonstrates selective molecular separation under capillary action alone, without any external energy input. As shown in Figure 6f, the collected solution exhibits a clear red color, and its UV-Vis spectrum (Figure 6e) reveals nearly complete retention of the RhB absorption peakalongside the total absence of the MB peak. This indicates that MB is efficiently captured during transport, while RhB passes freely through the framework. These results highlight the capability of the $Ag_2Mo_3O_{10}·1.8H_2O$/CFC hybrid to achieve continuous, selective separation of dissolved molecules in a flow-through configuration, leveraging its intrinsic capillary-driven transport and specific affinity for methylene blue.

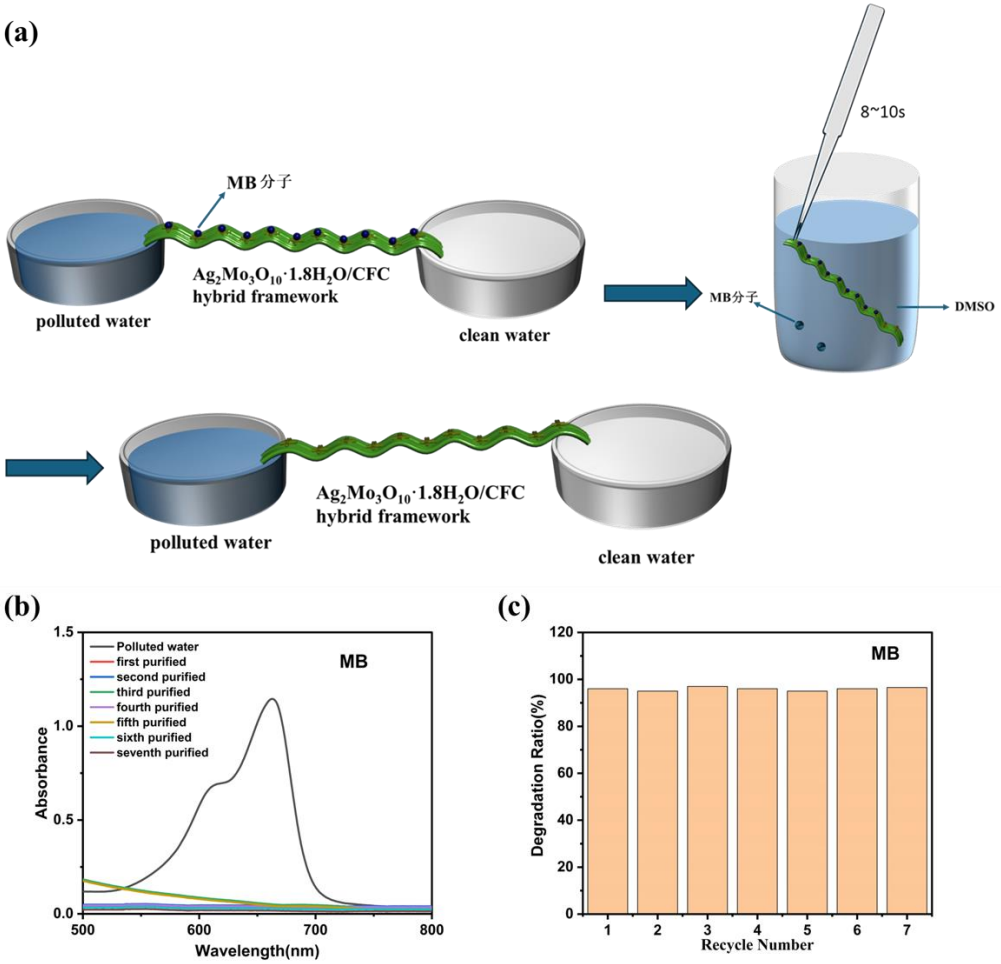

Figure 7. (a) Schematic diagram of material recycling and reuse. (b) UV-Vis absorption spectra of several recycle of MB. (c) Recovery of MB efficiency for seven times use.

Figures 7a-c demonstrate the reusability of the $Ag_2Mo_3O_{10}·1.8H_2O$/CFC hybrid framework, a crucial feature for practical application. The high selectivity toward methylene blue (MB) originates from the specific Ag–S coordination between Ag sites in the nanowires and MB molecules [16]. Importantly, this interaction is reversible under mild conditions. A 6 × 4 cm hybrid framework was tested over multiple cycles. After each adsorption of MB, the material was regenerated by simply immersing it in dimethyl sulfoxide (DMSO) for only 8–10 seconds, during which the MB molecules

 doi:10.20944/preprints202512.2569.v1

readily desorbed. The framework was then reused in a fresh MB-containing solution. As shown in Figure 7b, the UV-Vis spectra of the purified water remain nearly identical across seven consecutive cycles, with the MB peak consistently absent. Correspondingly, the calculated removal efficiency remained above 97% throughout all cycles (Figure 7c). These results confirm that the $Ag_2Mo_3O_{10}·1.8H_2O$/CFC hybrid can be rapidly and effectively regenerated without losing its structural integrity or adsorption performance. The combination of high selectivity, capillary-driven operation, and excellent recyclability underscores the strong potential of this material for sustainable, energy-efficient separation and recovery of sulfur-containing molecules in continuous-flow systems.

4. Conclusions

In summary, we successfully developed a novel $Ag_2Mo_3O_{10}·1.8H_2O$/carbon fiber cloth (CFC) hybrid framework through the dense and uniform growth of $Ag_2Mo_3O_{10}·1.8H_2O$ nanowires over a large-area CFC substrate. The interwoven nanowire-carbon fiber architecture forms a hierarchical porous network rich in micro-/nano-channels, which functions as an efficient capillary-driven water transport platform, achieving a flow rate of 1875 $mL·h^{-1}·m^{-2}$. Owing to the specific Ag-S coordination interaction, the hybrid framework exhibits rapid and selective adsorption toward sulfur-containing molecules, removing 94% of methylene blue (10 mg/L) within 10 min. The material also demonstrates excellent selectivity in mixed-dye systems, along with outstanding reusability (~97% recovery after multiple cycles) and stability under varying environmental conditions. Furthermore, a continuous-flow resource recovery system based on this framework was implemented, enabling simultaneous water purification and targeted molecule recovery without external energy input. Collectively, these attributes position the $Ag_2Mo_3O_{10}·1.8H_2O$/CFC hybrid as a highly promising and scalable material for advanced water resource recovery applications.

Author contributions: Lei-Yang Xue and Chu-Ya Luo prepared the composite materials. Lei-Yang Xue conducted the powder adsorption experiments, hybrid framework molecule selective separation tests, and flowing water velocity tests. Lei-Yang Xue, Han-Mei Xu, Jia-Xin Hua and Xue Zhang performed the composite material characterization. Jun Wu and Lian-Wen Zhu was responsible for initiating the research and supervising the project. Lian-Wen Zhu wrote the paper. Lian-Wen Zhu reviewed the entire manuscript.

Funding: This research was funded by Major Humanities and Social Sciences Research Projects in Zhejiang higher education institutions, Grant Number: 2024QN020.

Institutional Review Board Statement: Not applicable.

Informed Consent Statement: Not applicable.

Data Availability Statement: The original contributions presented in this study are included in the article. Further inquiries can be directed to the corresponding authors.

Conflicts of Interest: The authors declare no conflicts of interest.

References

1. Zhang W, Zhang Z, et al. Laccase immobilized on nanocomposites for wastewater pollutants degradation: current status and future prospects[J]. Bioprocess and Biosystems Engineering, **2023**, 46: 1513-1531.
2. Chan- Shih S, Wu- Jung H. Improving the Performance of the Reverse Osmosis Process with Fiber filter and Ultrafiltration: Promoting Municipal Sewage Reclamation and reuse for Industrial Processes[J]. Sustainability. **2022**, 14(9): 5443-5443.
3. Wu-Chun D, Zhu-Kai D, Hu-Xin K, et al. Ozone microbubbles treatment with different gas-liquid mixing conditions and its application on printing and dyeing wastewater and Escherichia coli[J]. Desalination and Water Treatment, **2022**, 252: 400-407.
4. Aleksandra K, Izabela K. From Environmental Threat to Control: A Review of Technologies for Removal of Quaternary Ammonium Compounds from Wastewater[J]. Membranes. **2025**, 16(1), 1.
5. Yang F, Wang-Xing B. Research recap of membrane technology for tannery wastewater treatment: a review[J]. Collagen and Leather, **2023**, 5(24).

 doi:10.20944/preprints202512.2569.v1

6. Wang F, Hou- Xin Y. Preparation of Cu-MnO2/GO/PVDF Catalytic Membranes via Phase Inversion Method and Application for Separation Removal of Dyes[J]. Membranes. **2025**, 15(12): 384.
7. Xie- Ya W, Liu- Ze W, et al. Water Purification Efficiency and Membrane Fouling Behavior of Ceramic Membrane-Nanofiltration in Treating Water Treatment Plant Production Wastewater[J]. Membranes. **2025**, 15(12): 387.
8. Saheli R. Carbon Nanotube and Graphene Oxide-Based Polymer Nanocomposite Membranes for Oil–Water Separation—Recent Advances and Future Prospects[J]. ChemistrySelect. **2025**,10(48).
9. Mei Y, Su-Yan H, Li Z, Bai- Shi Q, Yuan- Meng Y, Li L, Yan Z, Wu J* and Zhu- Lian W*. BiOBr nanoplates@TiO2 nanowires/carbon fiber cloth as a functional water transport network for continuous flow water purification[J]. Dalton Transactions, **2017**, 46, 347.
10. Eoin P M, Alexa E, et al. Polymer/iron-oxide nanocomposite adsorbents for cycled magnetically-enabled extraction of aqueous micropollutants[J]. RSC Sustainability. **2025**.
11. Ahmah R, Saeedeh H, et al. Retraction notice to "Preparation and characterization of nano composites from metal oxides and activated carbon from banana peel (MO@BPAC, MO=NiO, CuO and ZnO) for 2 nitrophenol removal from aqueous solutions[J]. Heliyon. **2025**, 11(1): e41245.
12. Muni R, Sumalatha B. A prototype integrated approach for sustainable treatment of organic dyes system using ZnO–CuO–AgO heterostructure as photocatalyst[J]. Scientific Reports. **2025**.
13. Vahid H, Gholamreza K and Dariush M. High-efficiency removal of methyl orange from wastewaters using polyimide/chitosan-MoS2-UiO-66 nanofiber adsorbents[J]. Scientific Reports. **2025**.
14. Tu C, Le T. g-C3N4 Nanosheet/ZnO Nanosponge Heterojunctions for Efficient Visible-Light Photocatalytic Degradation of Methylene Blue[J]. ChemNanoMat. **2025**.
15. Tu-Wen J, Cai-Wei Q. Selective adsorption of hazardous substances from wastewater by hierarchical oxide composites: A review[J]. Toxics, **2024**, 12: 447.
16. Xu-Ke Y, Wang L, Zhang-Yu X, et al. Graphene oxide enabled self-assembly of silver trimolybdate nanowires into robust membranes for nanosolid capture and molecular separation[J]. Nanoscale, **2023**, 15(14): 6607-6618.
17. Jing Z, Victoria S. C. Adsorption of octahedral mono-molybdate and poly-molybdate onto hematite: A multi-technique approach[J]. Journal of Hazardous Materials. **2022**, 431: 128564.
18. Yang L, Hong Z H, Wu J, et al. RSC Advances, **2014**, 4: 25556. H.K. Singh, K.V. Yeole, S.T. Mhaske. Synthesis and characterization of layer-by-layer assembled magnesium zinc molybdate nanocontainer for anticorrosive application[J]. Chemical Engineering Journal. **2016**,7: 414-426.
19. Young-Jung H, Mira P, Woo-Seok K, Kyong-Yop R, Soo-Jin P. Preparation and characterization of carbon black/pitch-based carbon fiber paper composites for gas diffusion layers[J]. Composites Part B, **2019**,159: 362–368.
20. Huang- Shan C, Ye J, Su- Mi M, Zhang Y, Meng Y, Meng X, Xia- Xin X. Efficient preparation and characterization of carbon fiber paper using phenolic resin in-pulp addition method[J]. International Journal of Hydrogen Energy. **2024**, 71: 506–514.
21. Vipin K, Sebastian M, et al. Design of Mixed-Metal Silver Decamolybdate Nanostructures for High Specific Energies at High Power Density[J]. Advanced Materials. **2016**,8: 6966-6975.
22. S. J. Pennycook and P. D. Nellist, Scanning transmission electron microscopy: imaging and analysis[J]. Springer, Berlin, 2011.
23. Yang- Xiang L, Wang Y, Xu X, Qu Y, Ding X, Chen H. Surface plasmon resonance-induced visible-light photocatalytic performance of silver/silver molybdate composites[J]. Chinese Journal of Catalysis. **2017**, 38: 260–269.
24. J.V.B. Moura, W.C. Ferreira, J.G. da Silva-Filho, F.G. Alabarse, P.T.C. Freire, C. Luz-Lima. $Ag_2Mo_3O_{10}$ nanorods under high pressure: In situ Raman spectroscopy[J]. Spectrochimica Acta Part A: Molecular and Biomolecular Spectroscopy. **2023**, 299: 122871.
25. G Nagaraju, G.T.Chandrappa and J Livage. Synthesis and characterization of silver molybdate nanowires, nanorods and multipods[J]. Bulletin of Materials Science. **2008**,31(3): 367–371.

 doi:10.20944/preprints202512.2569.v1

26. Jiang- De M, Chen- Hui N, Xie H, Cheng K, Li L, Xie K, Wang- Yu Q. Fe, N, S co-doped cellulose paper carbon fibers as an air-cathode catalyst for microbial fuel cells[J]. Environmental Research. **2023**, 221: 115308.
27. Joel- Marcos S, Assad U. K., Liu- Tian Y, Xu Z, Alan R. E., Liu- Guo L. Capacitive Organic Dye Removal by Block Copolymer Based Porous Carbon Fibers[J]. Advanced Materials Interfaces. **2020**.
28. Zhang- Shou W, Yang- Hong C, Huang- Hui Y, Gao- Hui H, Wang- Xiang X, Cao- Ru Y, Li- Jia X, Xu- Xi J, Wang- Xiang K. Unexpected ultrafast and high adsorption capacity of oxygen vacancy-rich WOx/C nanowire networks for aqueous Pb2+ and methylene blue removal Journal of Materials[J]. Chemistry A. **2017**. 1-11.
29. Qu- Tong Q, Huang- Xi Y, and Wang B. Effects of the Surface Structure on the Water Transport Behavior in PEMFC Carbon Fiber Papers[J]. ACS Omega **2022**, 7, 5992−5997.
30. A.N.C. Ferreira, W.C. Ferreira, A.V. Duarte. In situ high-temperature Raman scattering study of monoclinic Ag2Mo2O7 microrods[J]. Spectrochimica Acta Part A: Molecular and Biomolecular Spectroscopy. **2023**, 295: 122632.
31. Maria K do Nascimento- Silva L, João V.B.M. Silver Trimolybdate ($Ag_2Mo_3O_{10}.2H_2O$) Nanorods: Synthesis, Characterization, and Photo-Induced Antibacterial Activity under Visible-Light Irradiation[J]. Bioinorganic Chemistry and Applications. **2024**.